Supplementary Information for:

Calculations of the effect of catalyst size and structure on the electrocatalytic reduction of CO_2 on Cu nanoclusters

Geoffrey R. Weal,[a,b] Kristinn Ingi Guðmundsson,[c] Frank D. Mackenzie,[a,b] John R. Whiting,[a,b] Nicholas B. Smith,[a,b] Egill Skúlason,[c] and Anna L. Garden*[a,b]

[a] *Department of Chemistry, University of Otago, P.O. Box 56, Dunedin 9054, New Zealand.*
[b] *The MacDiarmid Institute for Advanced Materials and Nanotechnology, Victoria University of Wellington, P.O. Box 600, Wellington 6140, New Zealand.*
[c] *Science Institute and Faculty of Industrial Engineering, Mechanical Engineering and Computer Science, University of Iceland, VR-III, 107 Reykjavík, Iceland.*

anna.garden@otago.ac.nz

Contents

1 RGL potential for describing cluster energies in global optimisation

Cluster energies in the global optimisation were described with the Rosato-Guillopé-Legrand (RGL) potential:

$$E_{cluster} = \sum_{i=1}^{N} \{E_i^{rep} + E_i^{att}\} \tag{1}$$

$$E_i^{rep} = \sum_{j \neq i}^{N} A e^{-p\left(\frac{r_{ij}}{r_0} - 1\right)} \tag{2}$$

$$E_i^{att} = -\left[\sum_{j \neq i}^{N} \xi^2 e^{-2q\left(\frac{r_{ij}}{r_0} - 1\right)}\right]^{\frac{1}{2}} \tag{3}$$

where r_{ij} is the distance between atoms i and j, and A, p, q, ξ, and r_0 are fitted parameters taken from Cleri and Rosato (Table S1).[1] While Cleri and Rosato set a cutoff radius for the RGL potential to the fifth nearest neighbour, we chose to extend the RGL cutoff radius to infinity (i.e. no cutoff radius was considered).

Table S1 The parameters used in the Rosato-Guillopé-Legrand (RGL) potential for Cu, as given by Cleri and Rosato[1].

p	q	A (eV)	ξ (eV)	r_0 (Å)
10.960	2.2780	0.0855	1.2240	2.556

2 Different rearrangements of the lining of partial shell icosahedral Cu_{101} and Cu_{124} clusters

Figures S1 and S2 show selected examples of partial shell icosahedral Cu_{101} and Cu_{124} clusters with rearranged atoms about the lining of the partial shell.

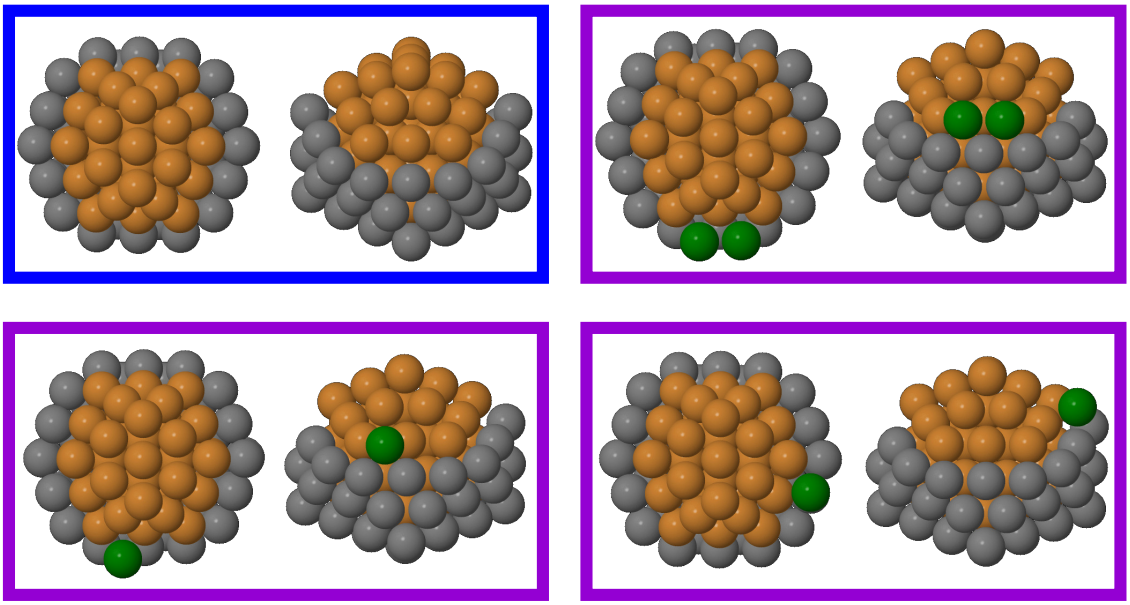

Figure S1 Various structures of the partial shell icosahedral Cu_{101} clusters with rearranged atoms about the lining of the shell. Selected examples of these rearranged partial shell icosahedral Cu_{101} clusters are given in purple boxes. The lowest energy partial shell icosahedral Cu_{101} cluster is given here in a blue box as a reference.

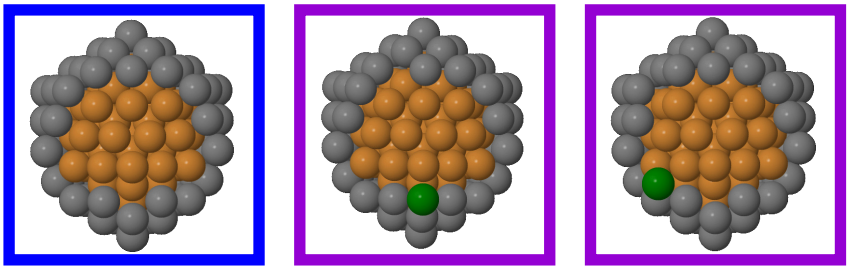

Figure S2 Various structures of the partial shell icosahedral Cu_{124} clusters with rearranged atoms about the lining of the shell. Selected examples of these rearranged partial shell icosahedral Cu_{124} clusters are given in purple boxes. The lowest energy partial shell icosahedral Cu_{124} cluster is given here in a blue box as a reference.

3 Relative energies of Cu clusters with adatoms or vacancies

Figures S3 to S5 show the relative energies of:

- various Cu_{54}, Cu_{55}, and Cu_{56} clusters (Figure S3),
- various Cu_{77}, Cu_{78}, and Cu_{79} clusters (Figure S4), and
- various Cu_{144}, Cu_{147}, and Cu_{150} clusters (Figure S5).

The energies of these Cu clusters have been relative to their perfect, closed-shell icosahedral form or the lowest energy form of I_h with a partial icosahedral shell.

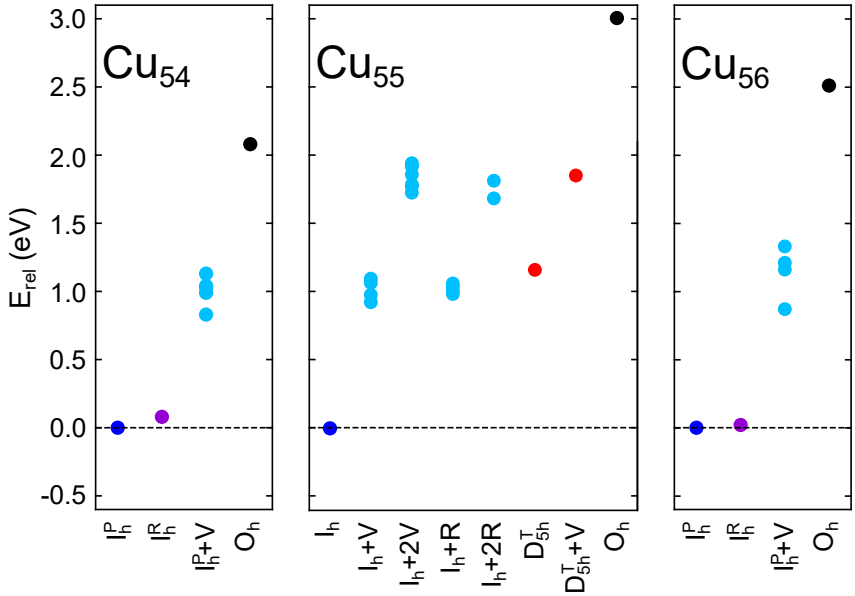

Figure S3 DFT energies of various Cu_{54}, Cu_{55}, and Cu_{56} clusters. The energies are all given relative to the perfect, closed shell icosahedral Cu_{55} cluster, or the lowest energy partial shell icosahedral Cu_{54} or Cu_{56} cluster. I_h: The perfect, closed-shell icosahedral cluster; $I_h{}^P$: The lowest energy form of I_h with a partial icosahedral shell; $I_h{}^E$: The elongated icosahedral cluster; $I_h{}^R$: I_h with a rearranged partial icosahedral shell; V: A vacant site; R: A rosette reconstruction; $D_{5h}{}^T$: A perfect, closed-shell twisted decahedral cluster; O_h: Versions of the octahedral motif.

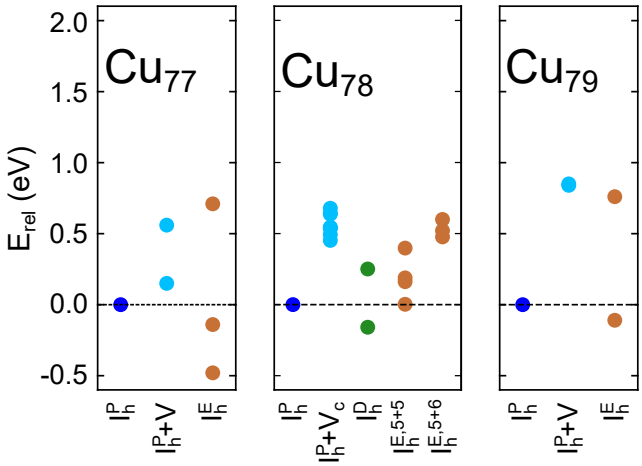

Figure S4 DFT energies of various Cu_{77}, Cu_{78}, and Cu_{79} clusters. The energies are all given relative to the lowest energy partial shell icosahedral Cu_{77}, Cu_{78}, or Cu_{79} cluster. $I_h{}^P$: The lowest energy form of I_h with a partial icosahedral shell; $I_h{}^R$: I_h with a rearranged partial icosahedral shell; $I_h{}^{E,5+5}$: The elongated icosahedral clusters with two five fold caps; $I_h{}^{E,5+6}$: The elongated icosahedral clusters with a five fold cap and a six fold cap; $I_h{}^D$: The distorted icosahedral clusters; V: A vacant site; V_c: A vacant corner site.

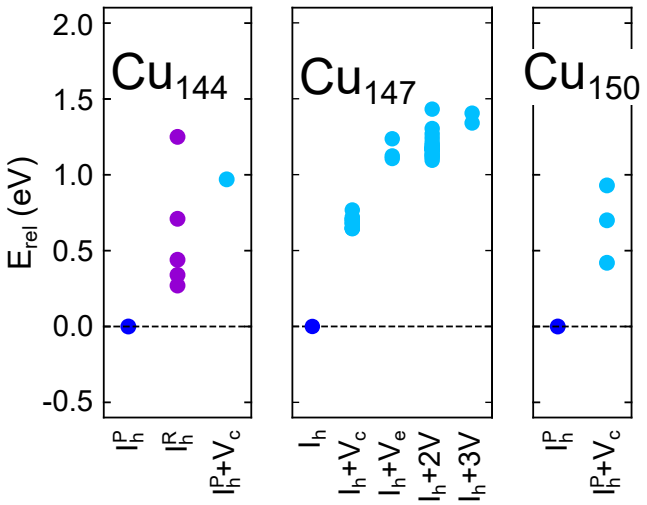

Figure S5 DFT energies of various Cu_{144}, Cu_{147}, and Cu_{150} clusters. The energies are all given relative to the perfect, closed shell icosahedral Cu_{147} cluster, or the lowest energy partial shell icosahedral Cu_{144} or Cu_{150} cluster. I_h: The perfect, closed-shell icosahedral cluster; $I_h{}^P$: The lowest energy form of I_h with a partial icosahedral shell; $I_h{}^R$: I_h with a rearranged partial icosahedral shell; V: A vacant site; V_c: A vacant corner site; V_e: A vacant edge site;

4 Adsorption energies and adsorption sites

Tables S2 to S4 show the energies and describe the site types for the lowest energy adsorption sites of intermediates upon various surfaces, respectively. Only the COOH, CO, and CHO site types and energies are given for $Cu_{78,c}$, $Cu_{54,cv}$, $Cu_{54,ev}$, $Cu_{56,6fc}$, and $Cu_{56,ad}$. Images of the lowest energy adsorption sites of intermediates upon the icosahedral Cu_{55} and Cu_{147} clusters, as well as on $Cu_{78,a}$ and $Cu_{78,b}$, are shown in Figures S6 to S10.

Table S2 Adsorption energies of intermediates upon various extended surfaces and Cu clusters. The lower the energy, the stronger the adsorbate binds to the surface of the Cu surface/cluster. All energies are given in eV.

Absorbate	Flat (111)	A Step (533)	B Step (553)	A edge	B edge	Cu_{55}	Cu_{147}	$Cu_{78,a}$	$Cu_{78,b}$	$Cu_{78,c}$
COOH[c]	0.76	0.46	0.48	0.52	0.50	0.49	0.47	0.38	-0.03	0.16
CO	0.98	0.81	0.82	0.91	0.86	0.71	0.94	0.60	0.64/0.68[b]	0.66
CHO	1.54	1.29	1.31	1.35	1.34	1.29	1.37	1.09	0.84	1.00
COH	2.12	2.08	2.13	1.98	2.17	2.02	2.33	1.78	1.89	
CH_2O	0.92[a]	0.91	0.92	0.98	0.95	0.90	1.07	0.71	0.78	
CHOH	1.80	1.39	1.43	1.54	1.56	1.67	1.71	1.50	1.18	
CH_3O	0.06	-0.10	-0.15	-0.10	-0.10	-0.05	-0.16	-0.44	-0.52	
CH_2OH	1.06	0.71	0.78	0.83	0.82	0.82	0.86	0.64	0.35	
CH_3	0.16	-0.20	-0.17	-0.14	-0.15	-0.05	-0.14	-0.36	-0.53	
CH_2	1.11	0.94	0.91	1.02	1.05	0.92	1.01	0.66	0.63	
CH	1.68	1.32	1.66	1.23	1.69	1.35	1.74	1.17	0.93/1.16[b]	
C	3.05	2.16	2.97	2.06	2.61	2.49	2.83	2.08	1.91/2.26[b]	
OH	0.03	-0.20	-0.24	-0.27	-0.18	-0.12	-0.19	-0.51	-0.68	
O	0.72	0.61	0.51	0.48	0.55	0.54	0.52	0.17	0.38/0.50[b]	

[a]Did not bind.
[b]Two adsorption energies are given. The first is the adsorption energy for the strongest binding site. This binding site is located on the other side of the cluster from where the *COOH moiety initial adsorbs. The second is the adsorption energy of a preferable binding site near where the *COOH moiety initially adsorbs.
[c]-0.45 added to energy to account for the poor description of C=O bonds with DFT. [2]

Table S3 Site types of the lowest energy adsorption sites of intermediates on various extended surfaces and Cu clusters, corresponding to adsorption energies in Table S2.

Absorbate	Flat (111)	A step (533)	B step (553)	A edge	B edge	Cu_{55}	Cu_{147}	$Cu_{78,a}$	$Cu_{78,b}$	$Cu_{78,c}$
COOH	top-top	top-top	top-top	top-top	top-top	top-top	top-top	top-top	top-top	top-top
CO	top	top	top	top	top	top (corner)	top (corner)	hollow	bridge/bridge[b]	top
CHO	top	top	top	top	top	top (C)	top (C)	bridge	top	top-top
COH	FCC	4-fold	FCC	4-fold	FCC	HCP	HCP	hollow	HCP	
CH_2O	DNB[a]	top-top	top-top	top-top	top-top	top (corner)	top (corner)	bridge-top	top	
CHOH	bridge	bridge	bridge	bridge	bridge	bridge	bridge	bridge	bridge	
CH_3O	FCC	bridge	bridge	bridge	bridge	HCP	HCP	hollow	bridge	
CH_2OH	top	top	top	top	top	top (C)	top (C)	top	top	
CH_3	bridge	bridge	bridge	bridge	bridge	bridge	top (corner)	bridge	bridge	
CH_2	FCC	bridge	bridge	bridge	bridge	HCP	bridge	hollow	bridge	
CH	FCC	4-fold	FCC	4-fold	FCC	dist. 4-fold	dist. 4-fold	4-fold	4-fold/4-fold[b]	
C	FCC	4-fold	bridge	4-fold	4-fold	dist. 4-fold	dist. 4-fold	4-fold	4-fold/4-fold[b]	
OH	FCC	bridge	bridge	bridge	bridge	HCP	HCP	hollow	bridge	
O	FCC	HCP	FCC	4-fold	FCC	HCP	HCP	hollow	hollow/4-fold[b]	

[a]Did not bind.
[b]Two adsorption energies are given. The first is the adsorption energy for the strongest binding site. This binding site is located on the other side of the cluster from where the *COOH moiety initial adsorbs. The second is the adsorption energy of a preferable binding site near where the *COOH moiety initially adsorbs.

Table S4 Adsorption energies (in eV) and site types of the lowest energy adsorption sites of intermediates on various Cu_{54} and Cu_{56} clusters. Here "cv" and "ev" refer to clusters with a corner and edge vacancy, respectively, "6fc" is a six-fold corner and "ad" is an adatom.

Absorbate	$Cu_{54,cv}$	$Cu_{54,ev}$	$Cu_{56,6fc}$	$Cu_{56,ad}$
COOH	0.25 top-top	0.46 top-top	0.51 top-top	0.32 top-bridge
CO	0.62 bridge	0.72 top (next to vacancy site)	0.69 top	0.66 top (on adatom)
CHO	1.08 top	1.14 top (next to vacancy site)	1.13 bridge	1.28 top (on adatom)

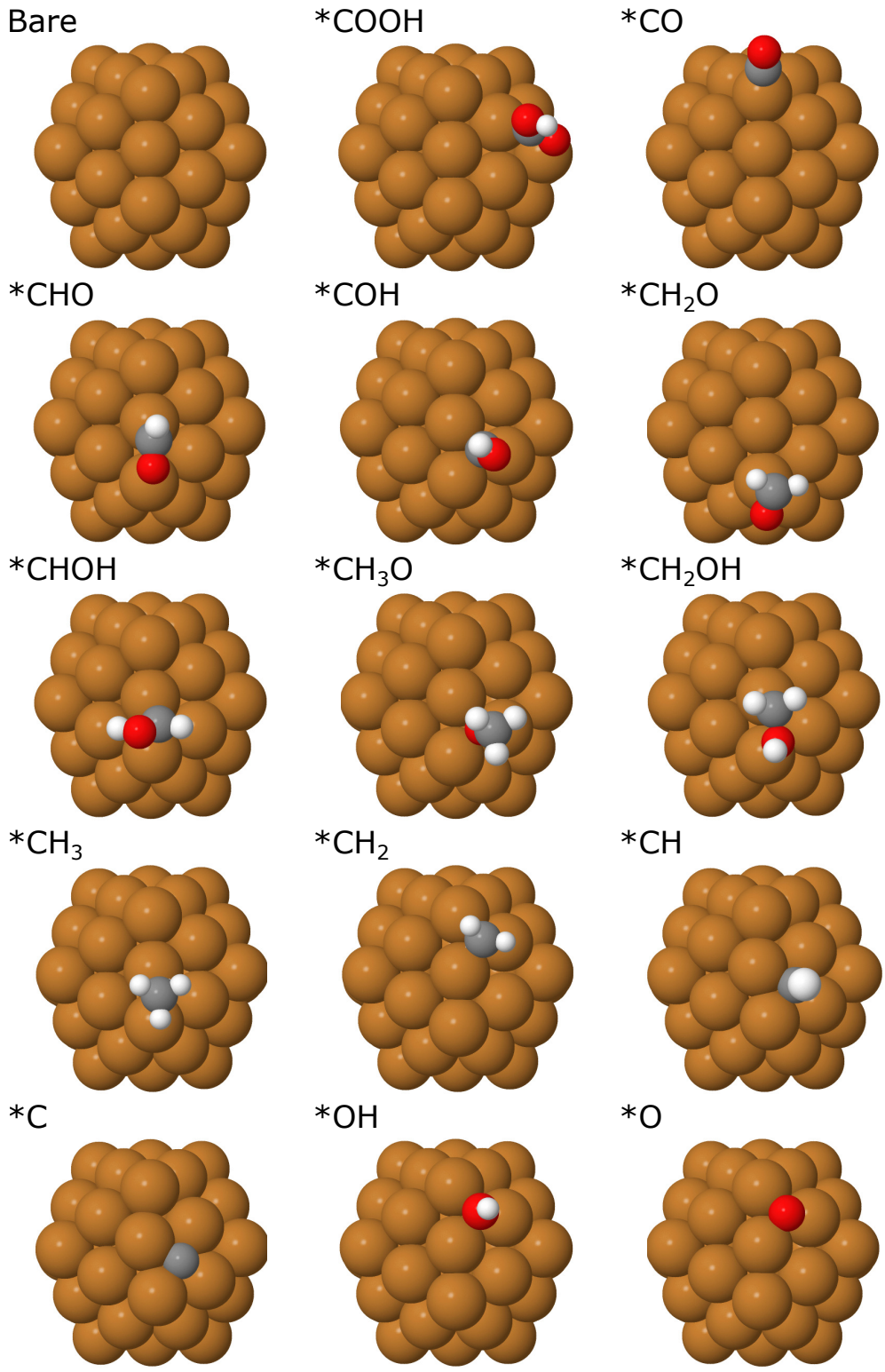

Figure S6 Lowest energy binding sites of adsorbates on the Cu_{55} cluster.

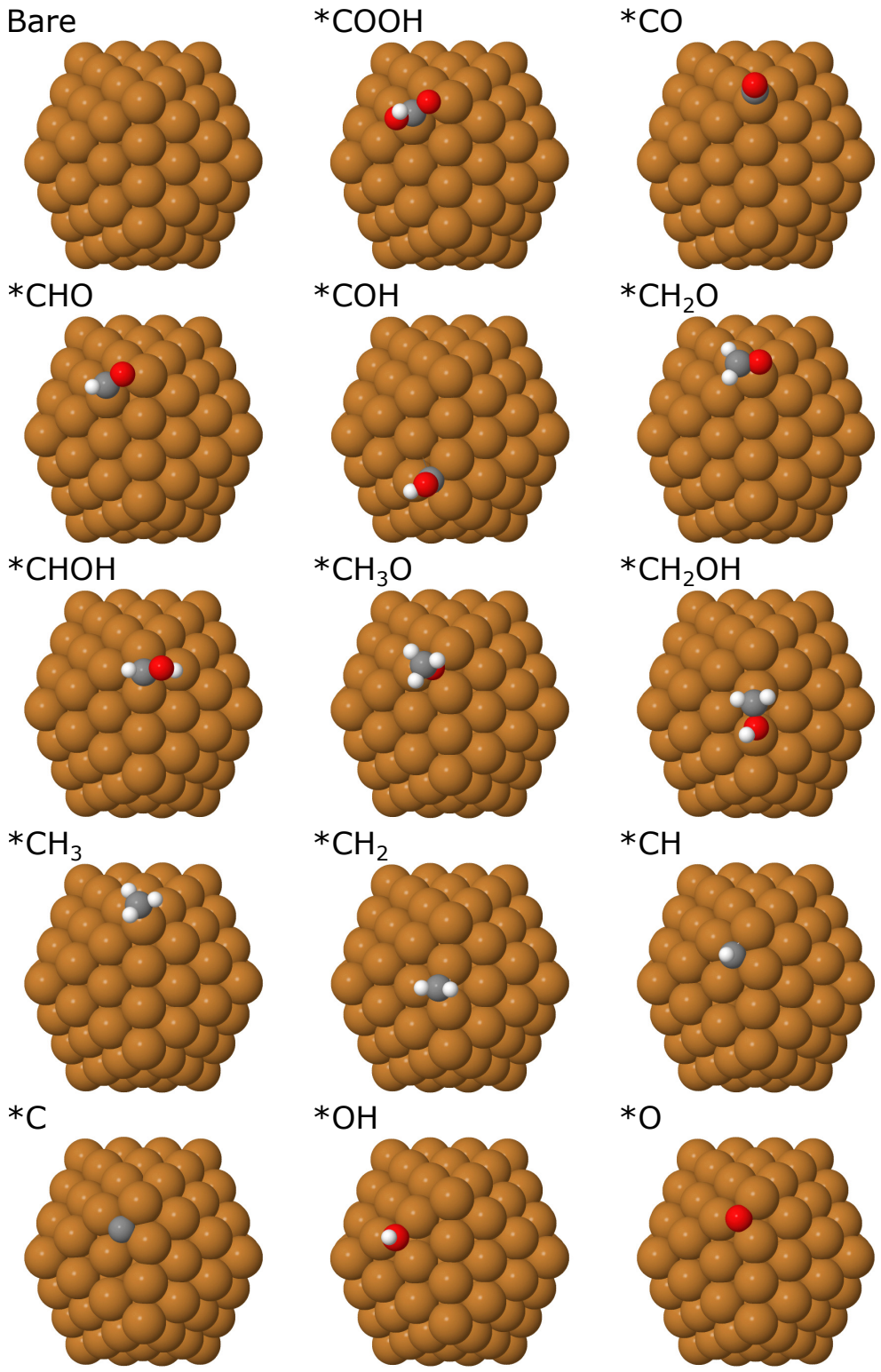

Figure S7 Lowest energy binding sites of adsorbates on the Cu_{147} cluster.

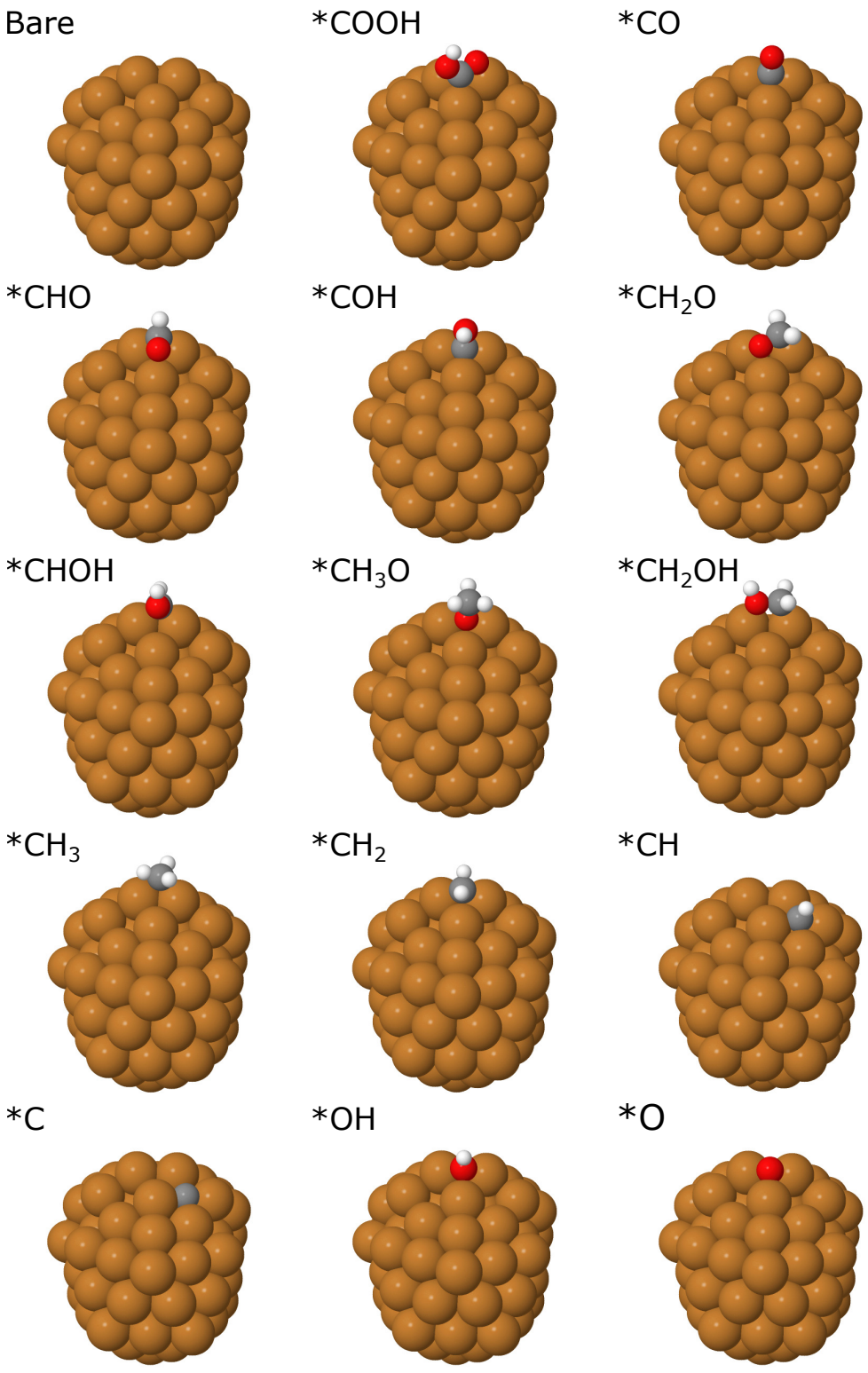

Figure S8 Lowest energy binding sites of adsorbates on the $Cu_{78,a}$ cluster.

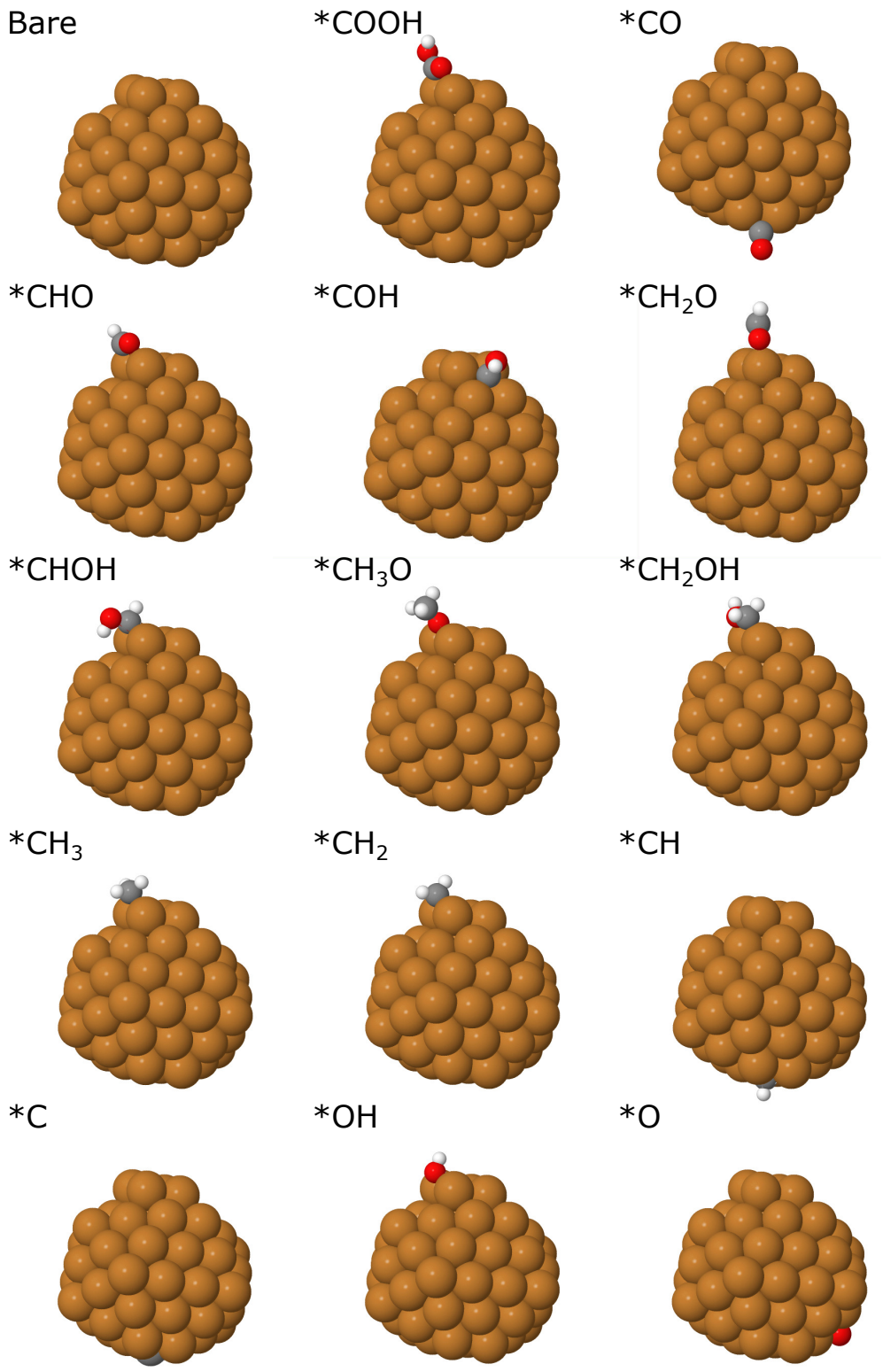

Figure S9 Lowest energy binding sites of adsorbates on the $Cu_{78,b}$ cluster.

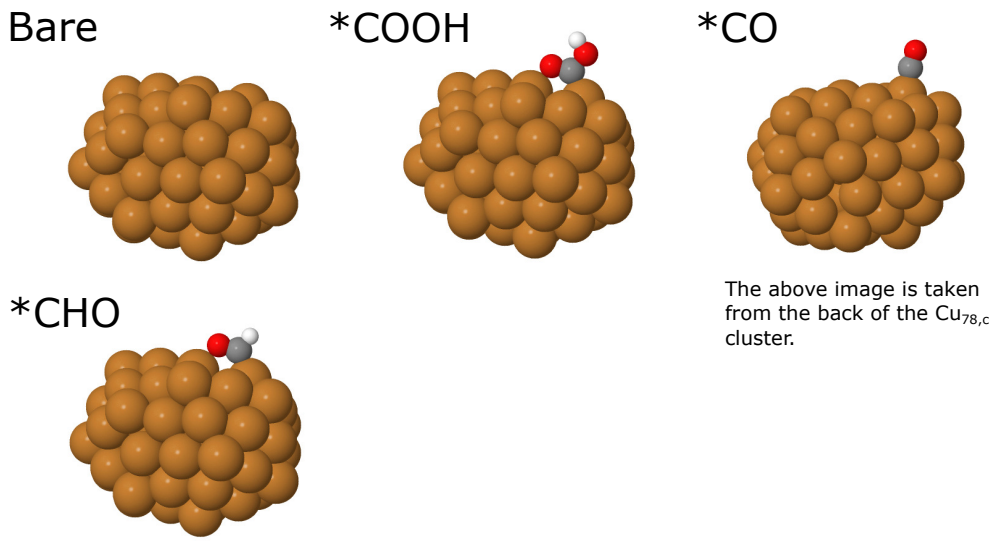

Figure S10 Lowest energy binding sites of adsorbates on the $Cu_{78,c}$ cluster. Only the bare cluster and the cluster with a *COOH, *CO, and *CHO adsorbate are shown. The image of the cluster with a *CO adsorbed to it is shown from the backside of the cluster.

5 Free energy diagrams of Cu surface models and clusters

The free energy diagrams at the limiting potential of A and B step surfaces, A and B edge surfaces, icosahedral Cu_{55} and Cu_{147} clusters, and $Cu_{78,a}$, $Cu_{78,b}$ and $Cu_{78,c}$ clusters, are shown in Figures S11 to S19.

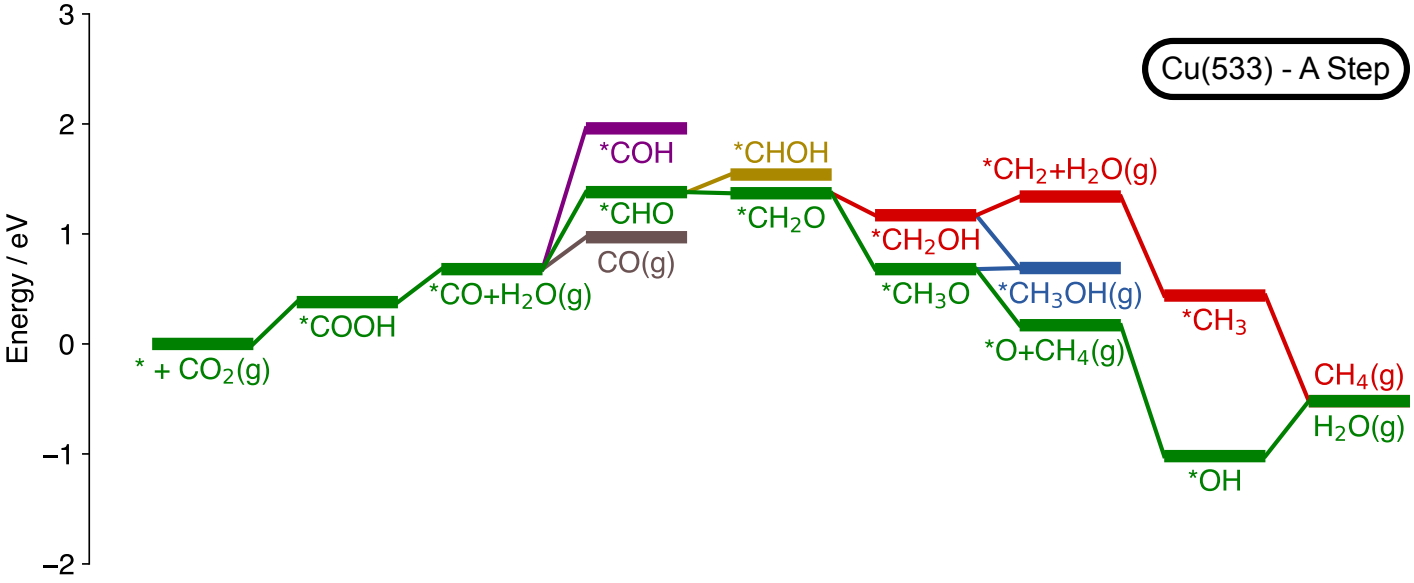

Figure S11 Free energy diagram for the reduction of CO_2 towards methane, methanol and CO on an A step surface. * indicates the adsorption site.

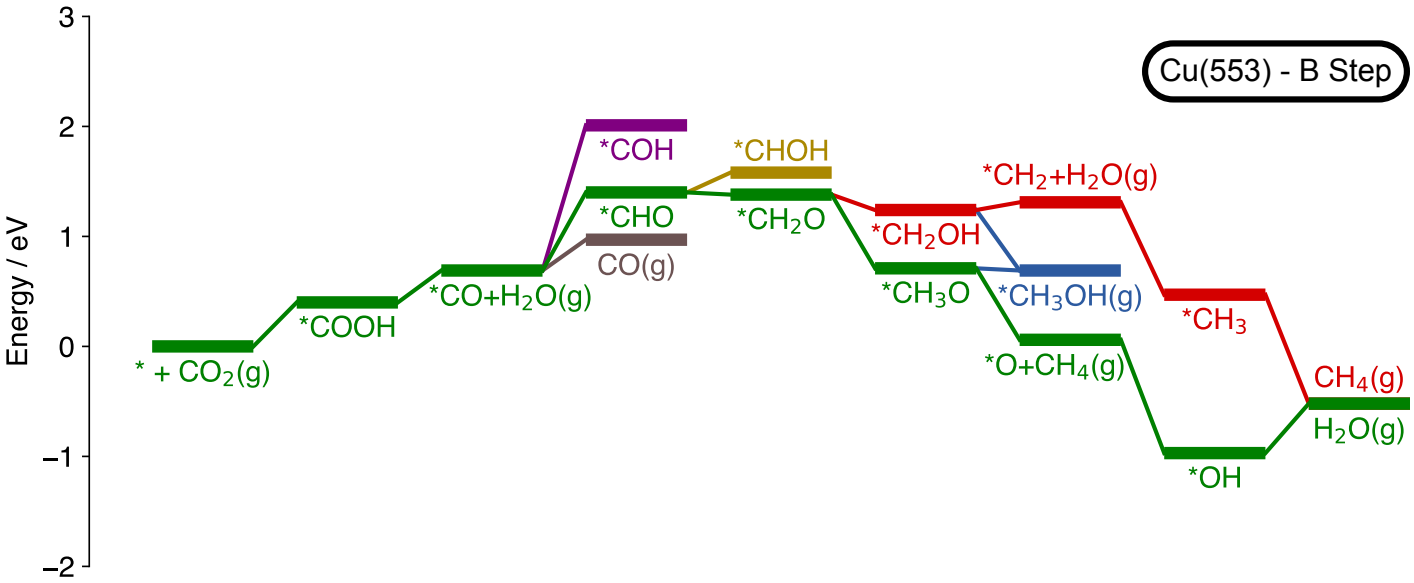

Figure S12 Free energy diagram for the reduction of CO_2 towards methane, methanol and CO on a B step surface. * indicates the adsorption site.

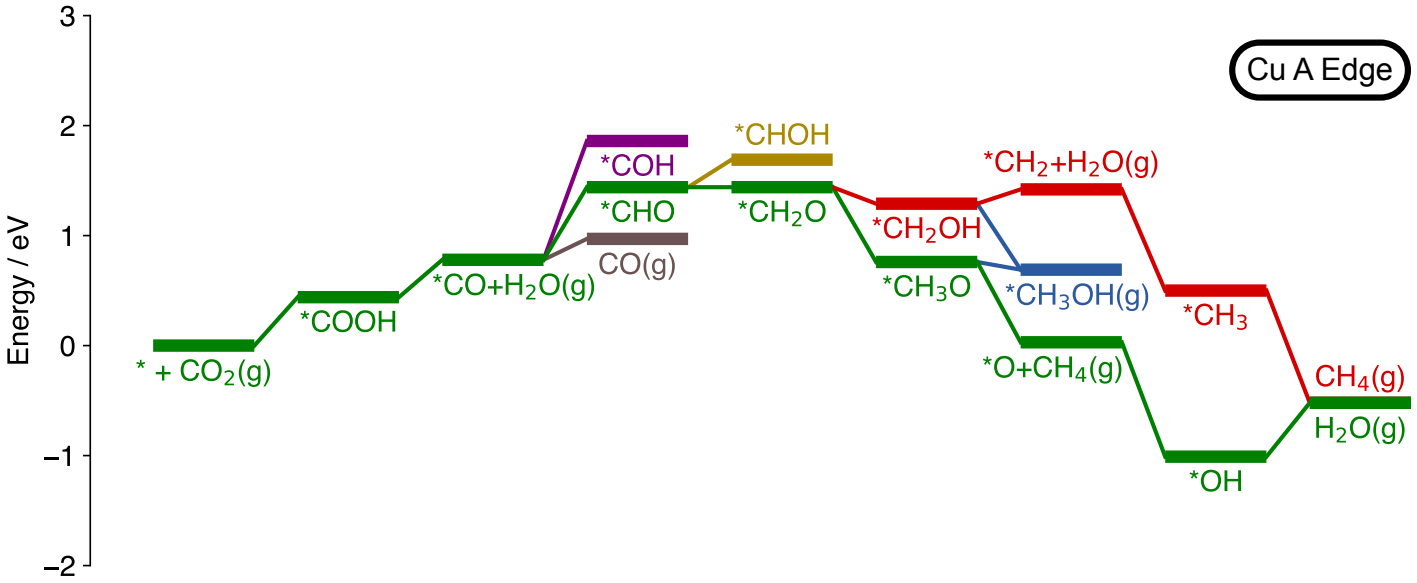

Figure S13 Free energy diagram for the reduction of CO_2 towards methane, methanol and CO on an A edge surface. * indicates the adsorption site.

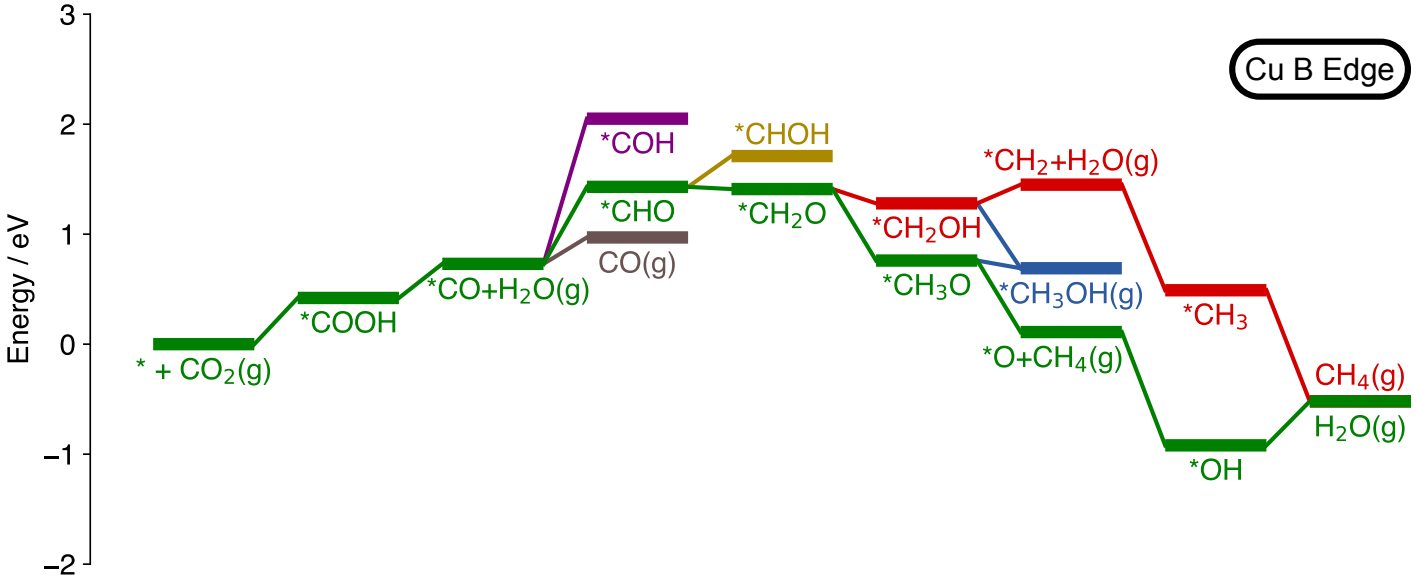

Figure S14 Free energy diagram for the reduction of CO_2 towards methane, methanol and CO on a B edge surface. * indicates the adsorption site.

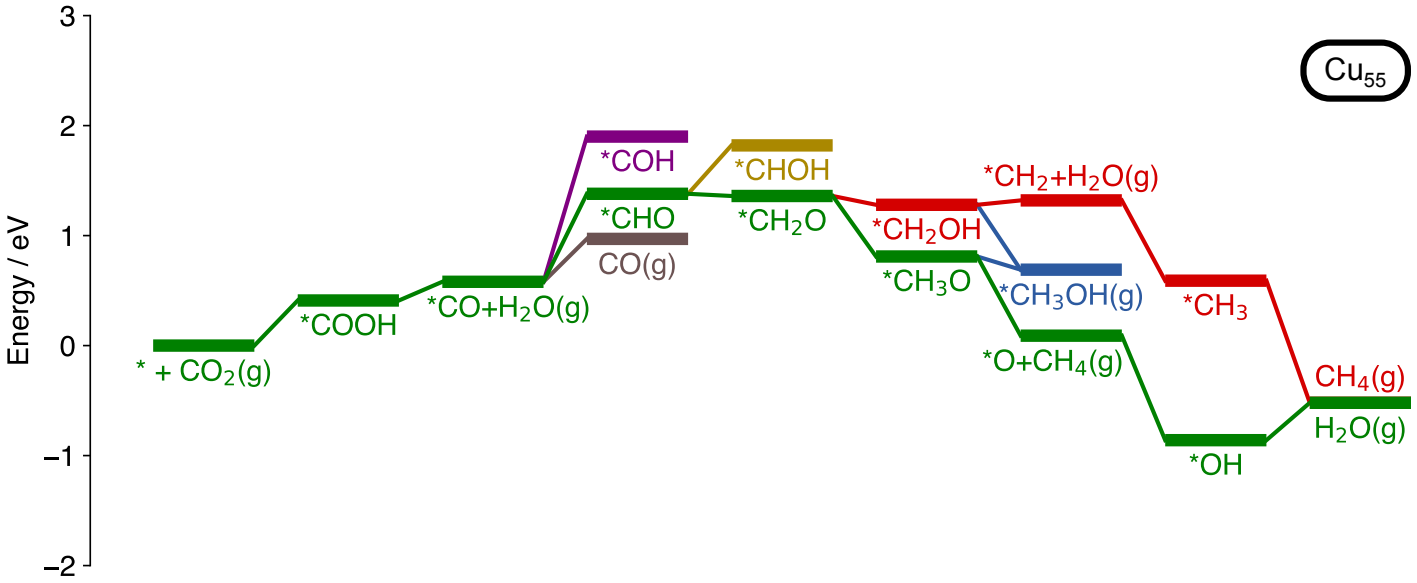

Figure S15 Free energy diagram for the reduction of CO_2 towards methane, methanol and CO on a Mackay Icosahedral Cu_{55} cluster. * indicates the adsorption site.

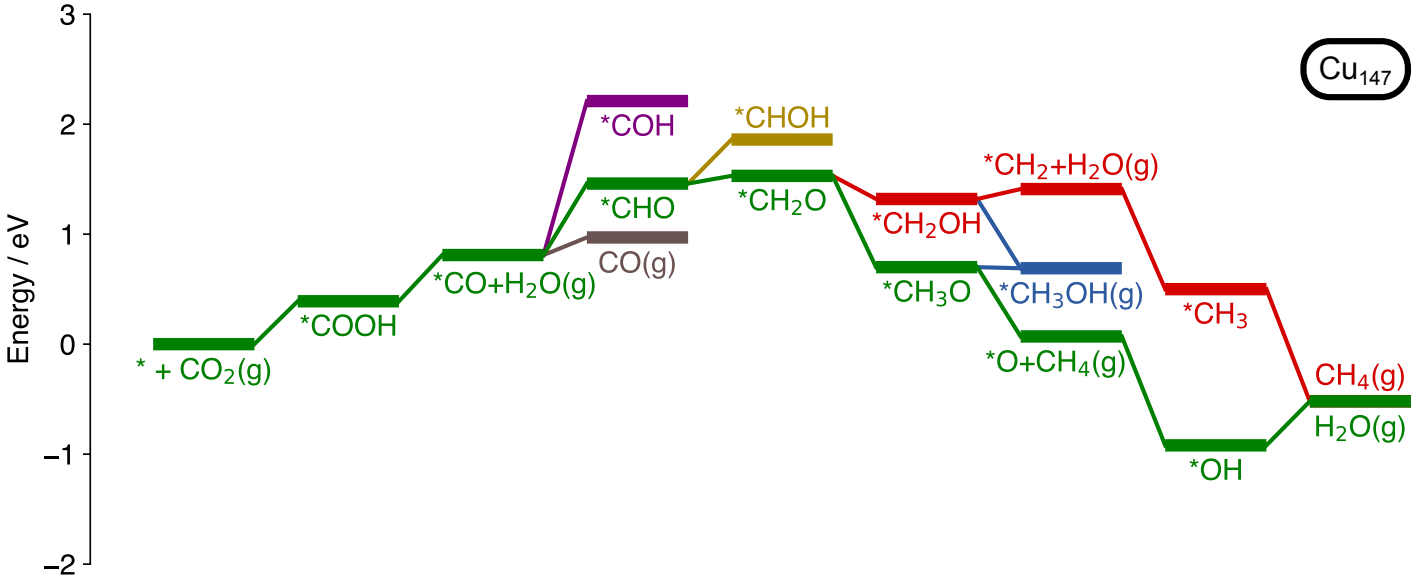

Figure S16 Free energy diagram for the reduction of CO_2 towards methane, methanol and CO on a Mackay Icosahedral Cu_{147} cluster. * indicates the adsorption site.

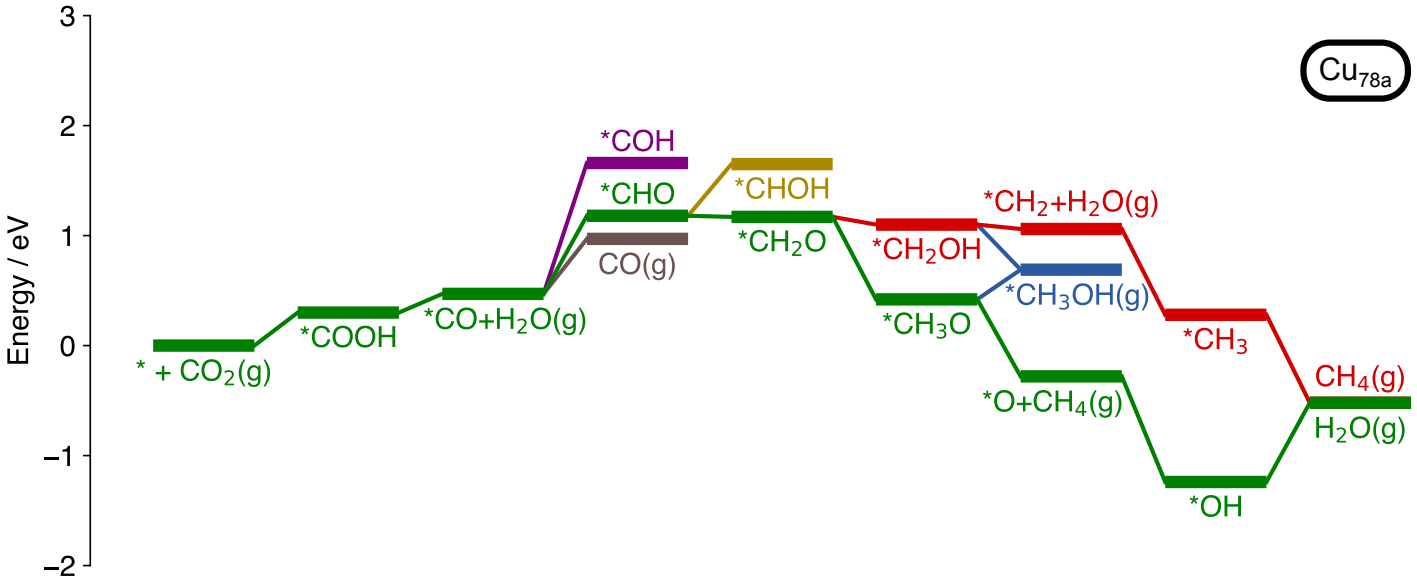

Figure S17 Free energy diagram for the reduction of CO_2 towards methane, methanol and CO on a partial shell $Cu_{78,a}$ cluster. * indicates the adsorption site.

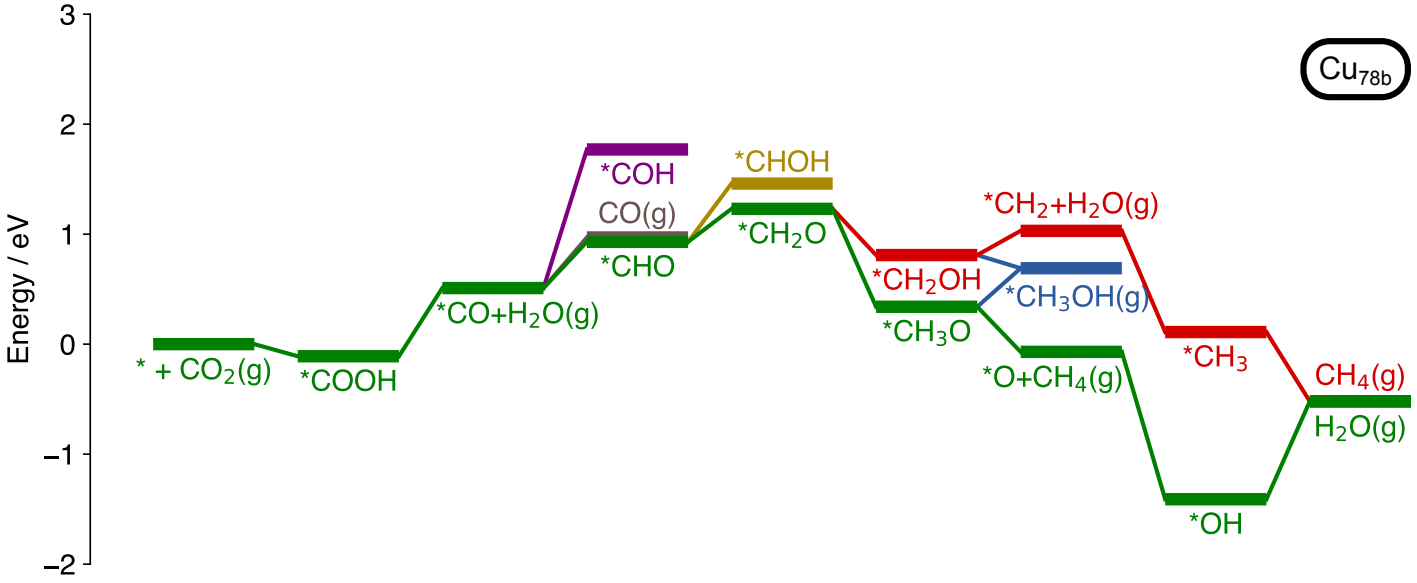

Figure S18 Free energy diagram for the reduction of CO_2 towards methane, methanol and CO on the elongated $Cu_{78,b}$ cluster. * indicates the adsorption site.

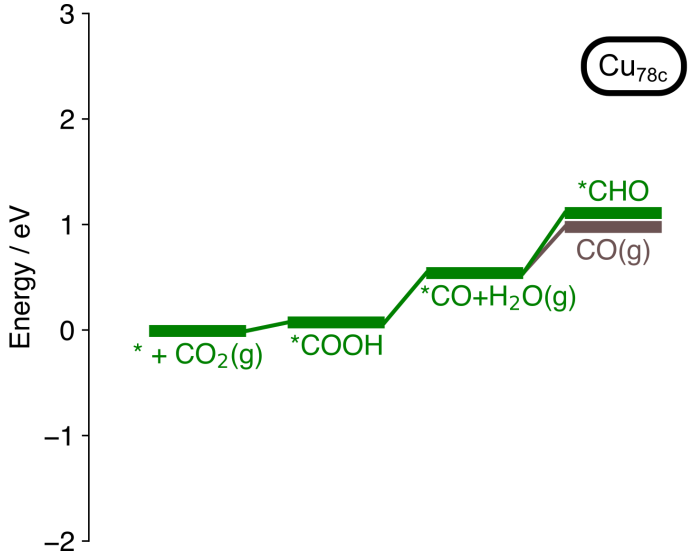

Figure S19 Free energy diagram for the reduction of CO_2 towards methane, methanol and CO on the distorted $Cu_{78,c}$ cluster. * indicates the adsorption site. Only the first three steps of this mechanism are given.

6 Free energy diagrams at calculated limiting potentials

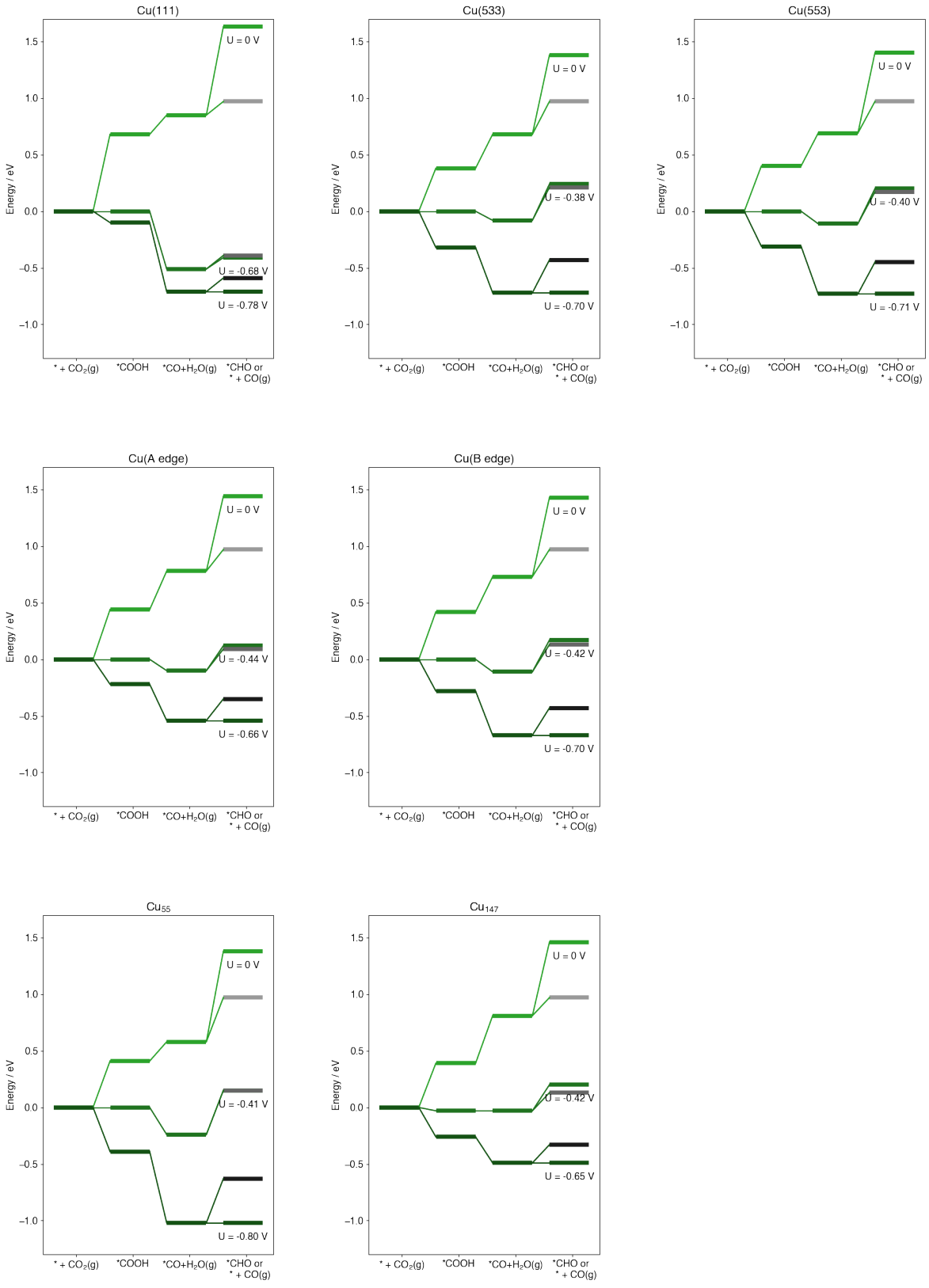

Figure S20 continued next page...

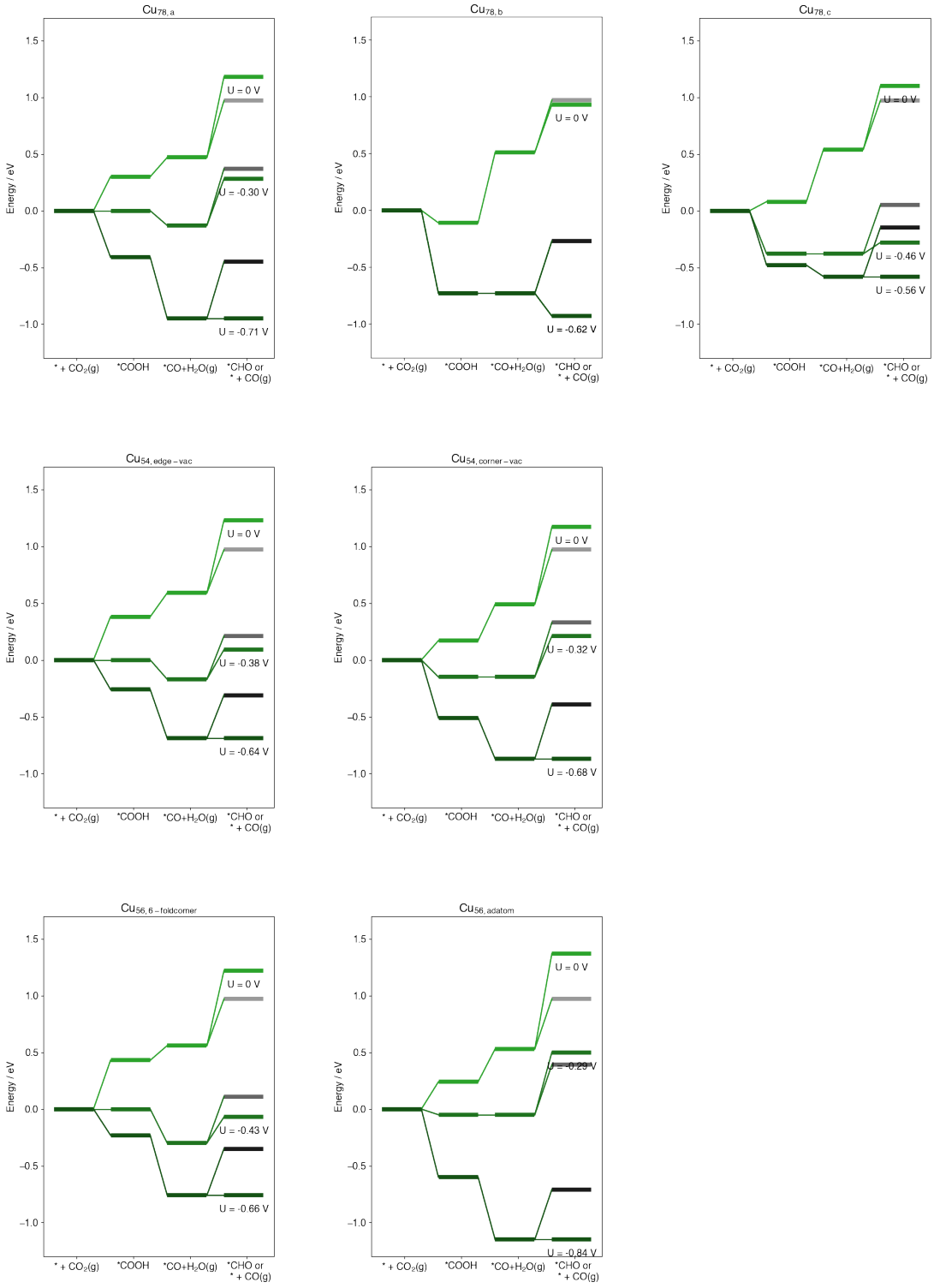

Figure S20 Free energy diagrams for CO_2RR to CO, CH_4 and CH_3OH at 0 V and at the calculated limiting potential for each product.

7 Structures of lowest energy off-size clusters

Figure S21 shows the lowest energy structures for off-size clusters, being $Cu_{54\text{-}56}$, $Cu_{77\text{-}79}$, and $Cu_{144\text{-}150}$.

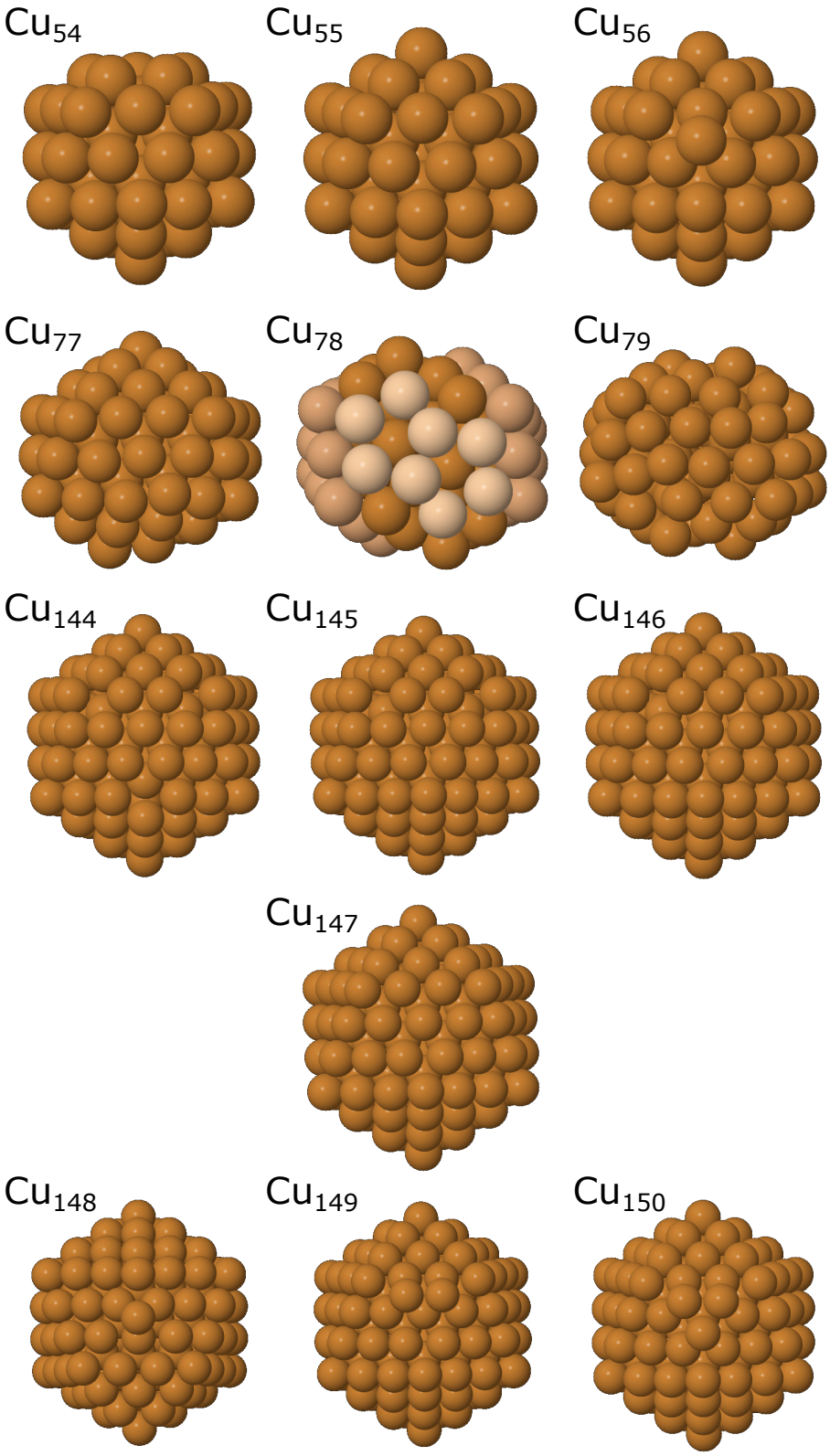

Figure S21 Global minima of Cu_{54}-Cu_{56}, Cu_{77}-Cu_{79}, and Cu_{144}-Cu_{150}, after being re-optimised with DFT (with the PBE functional).

8 Geometric parameters and Bader charges of *COOH

Table S5 COOH adsorption energy (E_{ads}), net Bader charge and selected geometric parameters for bare catalyst and COOH(g) ("Free") and catalyst with adsorbed COOH ("Ads.").

	E_{ads} / eV	Geometric parameters				Net Bader charge / e^-					
		R(Cu-Cu) / Å		R(C-O) / Å		Cu(C)		Cu(O)		COOH	
		Free	Ads.	Free	Ads.	Free	Ads.	Free	Ads.	Free	Ads.
Cu(111)	0.98	2.616	2.676	1.197	1.256	0.02	-0.13	0.02	-0.19	0	0.45
B edge	0.50	2.616	2.701	1.197	1.263	0.04	-0.14	0.04	-0.26	0	0.47
Cu_{55}	0.49	2.563	2.759	1.197	1.264	0.01	-0.14	0.06	-0.20	0	0.57
Cu_{147}	0.47	2.558	2.751	1.197	1.268	0.00	-0.16	0.05	-0.20	0	0.52
$Cu_{78,a}$[a]	0.38	N/A	N/A	1.197	1.272	0.01/0.01	-0.14/-0.09	0.05	-0.20	0	0.57
$Cu_{78,b}$	-0.03	2.491	2.784	1.197	1.268	0.04	-0.18	0.03	-0.25	0	0.50
$Cu_{78,c}$	0.16	3.085	3.260	1.197	1.261	0.01	-0.18	-0.01	-0.23	0	0.52

[a] COOH adsorbs with C bridging two Cu atoms for $Cu_{78,a}$

9 Density of states of *COOH

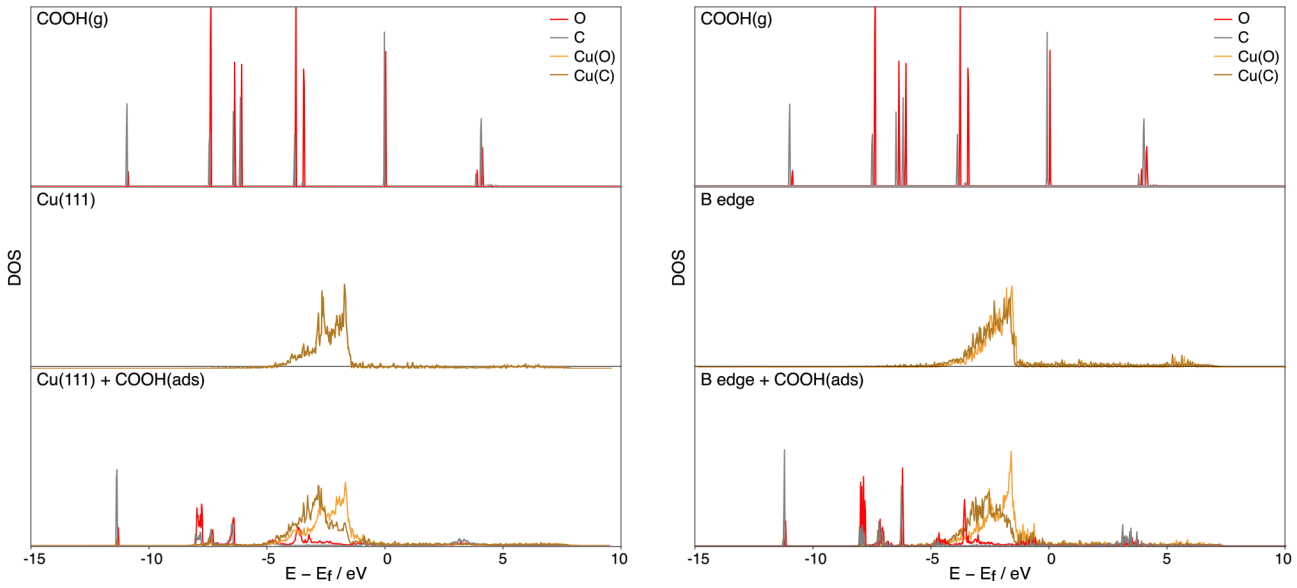

Figure S22 Density of states (DOS) for COOH(g) (top panel), bare Cu catalyst (middle panel) and combined system with COOH adsorbed on the catalyst (bottom) for Cu(111) (left) and B edge (right). DOS are projected onto the atoms of interest where Cu(C) indicates the Cu atom nearest to the C atom of COOH and Cu(O) indicates the Cu atom nearest to the carbonyl O atom.

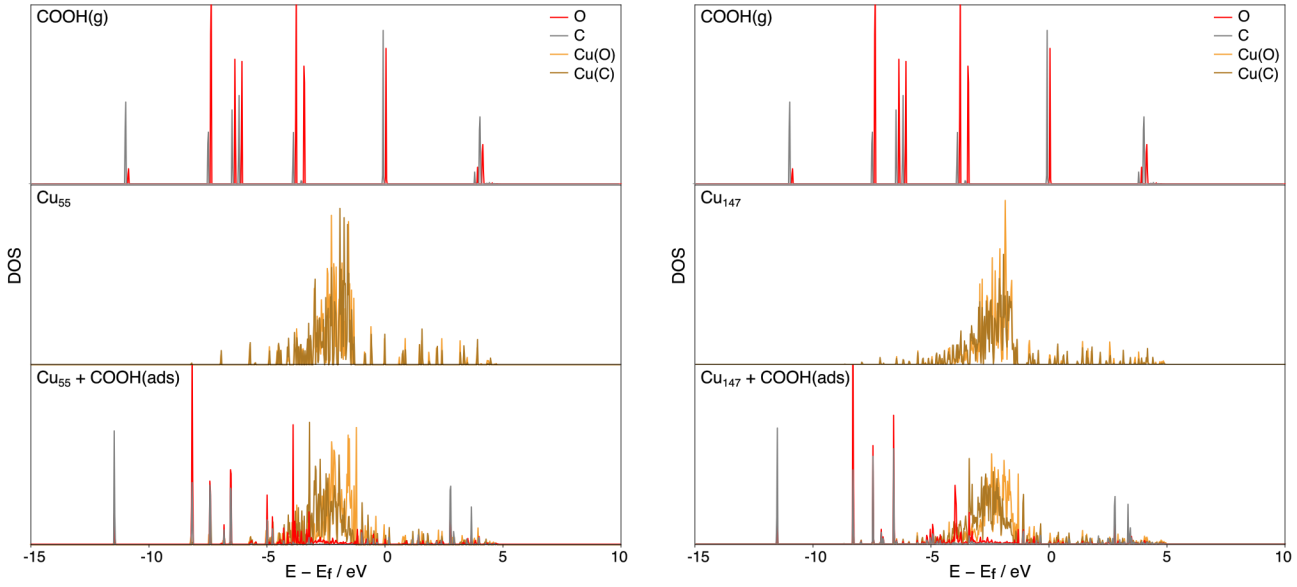

Figure S23 Density of states (DOS) for COOH(g) (top panel), bare Cu catalyst (middle panel) and combined system with COOH adsorbed on the catalyst (bottom) for Cu_{55} (left) and Cu_{147} (right). DOS are projected onto the atoms of interest where Cu(C) indicates the Cu atom nearest to the C atom of COOH and Cu(O) indicates the Cu atom nearest to the carbonyl O atom.

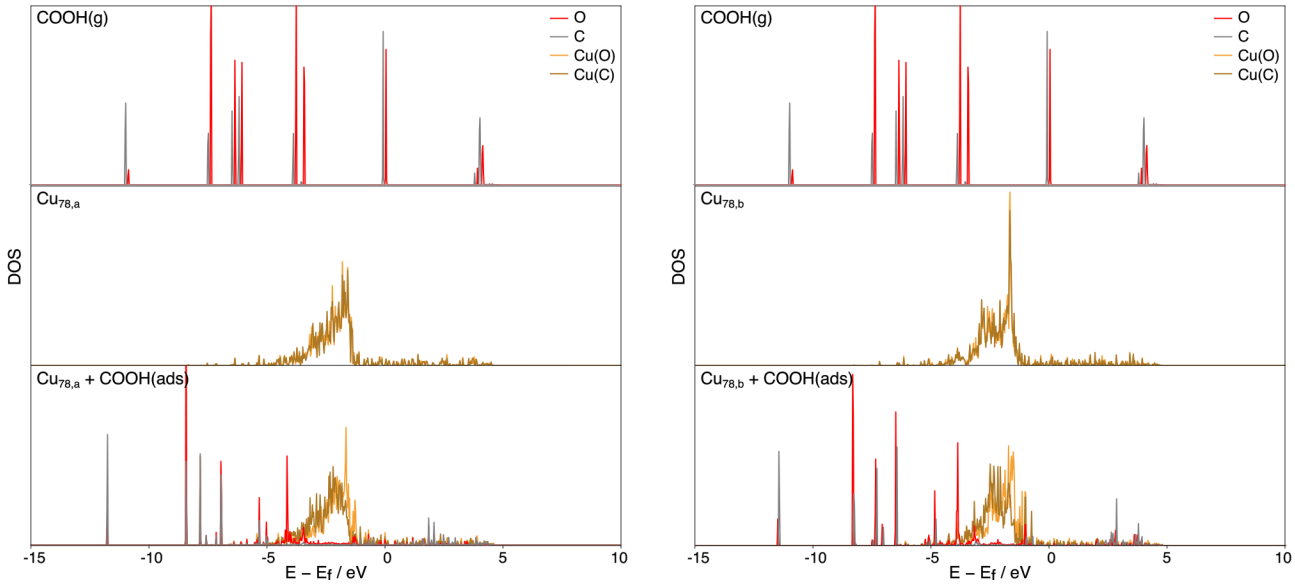

Figure S24 Density of states (DOS) for COOH(g) (top panel), bare Cu catalyst (middle panel) and combined system with COOH adsorbed on the catalyst (bottom) for $Cu_{78,a}$ (left) and $Cu_{78,b}$ (right). DOS are projected onto the atoms of interest where Cu(C) indicates the Cu atom nearest to the C atom of COOH and Cu(O) indicates the Cu atom nearest to the carbonyl O atom.

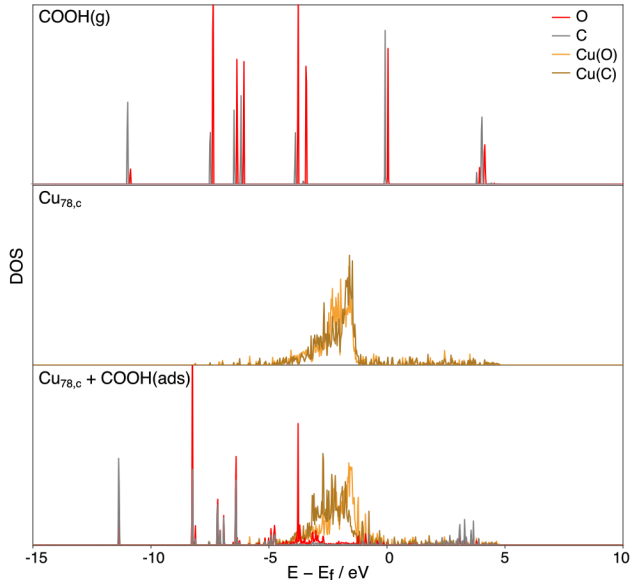

Figure S25 Density of states (DOS) for COOH(g) (top panel), bare Cu catalyst (middle panel) and combined system with COOH adsorbed on the catalyst (bottom) for $Cu_{78,c}$. DOS are projected onto the atoms of interest where Cu(C) indicates the Cu atom nearest to the C atom of COOH and Cu(O) indicates the Cu atom nearest to the carbonyl O atom.

Notes and references

[1] F. Cleri and V. Rosato, *Phys. Rev. B*, 1993, **48**, 22–33.

[2] A. A. Peterson, F. Abild-Pedersen, F. Studt, J. Rossmeisl and J. K. Norskov, *Energy Environ. Sci.*, 2010, **3**, 1311–1315.